Received: 14 April 2021 | Revised: 9 July 2021 | Accepted: 23 August 2021

DOI: 10.1111/epi.17061

Epilepsia®

FULL-LENGTH ORIGINAL RESEARCH

Accurate detection of typical absence seizures in adults and children using a two-channel electroencephalographic wearable behind the ears

Lauren Swinnen[1] | **Christos Chatzichristos**[2] | **Katrien Jansen**[3] | **Lieven Lagae**[3] | **Chantal Depondt**[4] | **Laura Seynaeve**[5,6] | **Evelien Vancaester**[7] | **Annelies Van Dycke**[8] | **Jaiver Macea**[1] | **Kaat Vandecasteele**[2] | **Victoria Broux**[1] | **Maarten De Vos**[2,3] | **Wim Van Paesschen**[1]

[1]Laboratory for Epilepsy Research, KU Leuven and Department of Neurology, University Hospitals, Leuven, Belgium

[2]Department of Electrical Engineering, STADIUS Center for Dynamical Systems, Signal Processing and Data Analytics, KU Leuven, Leuven, Belgium

[3]Department Development and Regeneration, KU Leuven, Leuven, Belgium

[4]Department of Neurology, Hôpital Erasme, Université Libre de Bruxelles (ULB), Brussels, Belgium

[5]Department of Neurology, Universitair Ziekenhuis Brussel (UZ Brussel), Brussels, Belgium

[6]Neuroprotection and Neuromodulation, Center for Neurosciences (C4N), Vrije Universiteit Brussel (VUB), Brussels, Belgium

[7]Department of Neurology, General Hospital Groeninge, Kortrijk, Belgium

[8]Department of Neurology, General Hospital Sint-Jan, Brugge, Belgium

Correspondence
Lauren Swinnen, Laboratory for Epilepsy Research, KU Leuven, UZ Herestraat 49, Leuven 3000, Belgium.
Email: lauren.swinnen@kuleuven.be

Funding information
Flemish Government (AI Research Program); EIT Health, Grant/Award Number: 21263 - SeizeIT2

Summary

Objective: Patients with absence epilepsy sensitivity <10% of their absences. The clinical gold standard to assess absence epilepsy is a 24-h electroencephalographic (EEG) recording, which is expensive, obtrusive, and time-consuming to review. We aimed to (1) investigate the performance of an unobtrusive, two-channel behind-the-ear EEG-based wearable, the Sensor Dot (SD), to detect typical absences in adults and children; and (2) develop a sensitive patient-specific absence seizure detection algorithm to reduce the review time of the recordings.

Methods: We recruited 12 patients (median age = 21 years, range = 8–50; seven female) who were admitted to the epilepsy monitoring units of University Hospitals Leuven for a 24-h 25-channel video-EEG recording to assess their refractory typical absences. Four additional behind-the-ear electrodes were attached for concomitant recording with the SD. Typical absences were defined as 3-Hz spike-and-wave discharges on EEG, lasting 3 s or longer. Seizures on SD were blindly annotated on the full recording and on the algorithm-labeled file and consequently compared to 25-channel EEG annotations. Patients or caregivers were asked to keep a seizure diary. Performance of the SD and seizure diary were measured using the F1 score.

Results: We concomitantly recorded 284 absences on video-EEG and SD. Our absence detection algorithm had a sensitivity of .983 and false positives per hour rate of .9138. Blind reading of full SD data resulted in sensitivity of .81, precision of .89, and F1 score of .73, whereas review of the algorithm-labeled files resulted in scores of .83, .89, and .87, respectively. Patient self-reporting gave sensitivity of .08, precision of 1.00, and F1 score of .15.

Significance: Using the wearable SD, epileptologists were able to reliably detect typical absence seizures. Our automated absence detection algorithm reduced the review time of a 24-h recording from 1-2 h to around 5–10 min.

KEYWORDS
epilepsy, seizure detection algorithm, seizure underreporting, typical absence seizures, wearable seizure detection

1 | INTRODUCTION

Typical absence seizures are episodes of sudden onset impairment of consciousness accompanied by regular and symmetrical 3-Hz spike-and-wave discharges (SWDs) on the electroencephalogram (EEG).[1] They appear in .7–4.6 of 100 000 individuals across the general population.[2] Typical absence seizures occur in three idiopathic generalized epilepsy syndromes, namely childhood absence epilepsy, juvenile absence epilepsy, and juvenile myoclonic epilepsy.[3]

Absence seizures place a burden on the patient's quality of life due to constraints experienced in daily life, for example, the inability to drive a car and difficulties experienced at school because of attention problems.[4] Prognosis and outcomes depend, among other things, on the type of epilepsy syndrome and the efficacy of the initial treatment.[5] Nevertheless, data on remission rates remain inconclusive (range = 51%–93%) due to sparse research and the use of heterogeneous classification criteria for the diagnosis of absence epilepsy as well as for remission.[6–8]

To optimize therapy, accurate seizure counting is paramount. Current diagnostics are based on clinical history, in-hospital monitoring of seizures with video-EEG, and seizure diaries kept by the patient. However, the latter poorly reflects the actual seizure frequency, as <50% of seizures are accurately reported by patients.[9] Absence seizures are often the most challenging seizure type to be correctly identified by caregivers, usually due to the lack of a visible clinical correlate.[10] Research showed that patients reported only 6% of all experienced absences,[11] whereas caregivers of children reported 14%.[10] Moreover, the use of gold standard video-EEG is limited to the hospital, is expensive, and does not allow for long-term monitoring.[9] Other strategies, such as ambulatory EEG, are not available everywhere, and can add to the stigma that people with epilepsy already have.[12]

Therefore, the market of wearable seizure detection devices has been growing steadily, but clinical adoption remains challenging.[13] EEG is the only biosignal that allows accurate detection of absences. EEG-based wearables have been previously developed, for example, the ear-EEG[14,15] and Epilog[16]; however, little research has been done into wearable detection of absence seizures. In addition to achieving high detection accuracy, wearables should also be designed to be unobtrusive, easy to wear, and nonstigmatizing.[17] Accurate logging of the frequency of seizures using a wearable would significantly contribute to patient management in the outpatient setting. Moreover, (semi-)automated seizure detection would facilitate adoption in clinical practice.

Key Points

- Absence seizures can be accurately detected using an unobtrusive two-channel EEG-based wearable, the Sensor Dot
- The vast amount of recorded EEG data can be reduced with an automated absence seizure detection algorithm
- Implementation of this algorithm suggests improved performance and reduces time needed to review a 24-h EEG from 1–2 h to 5–10 min

We report the performance of an EEG-based wearable device detecting absence seizures. This CE-marked device, the Sensor Dot (SD; Byteflies), is a discrete,[18] user-friendly wearable that makes use of two behind-the-ear channels to detect seizures. This device was developed during SeizeIT1 (2016–2019). The current study is an extension of SeizeIT1 and part of a larger multicenter trial in which we focus on clinical validation of the SD in people with typical absence, focal impaired awareness, and generalized tonic–clonic seizures (EIT Health: SeizeIT2; clinicaltrials.gov: NCT04284072).[19]

2 | MATERIALS AND METHODS

2.1 | Patients

Patients who were admitted to the epilepsy monitoring unit (EMU) for 24-h routine video-EEG monitoring to investigate refractory absence epilepsy, were recruited at University Hospital Leuven (UZ Leuven), Leuven, Belgium, between October 23, 2019 and February 24, 2020. Patients were included if they had refractory idiopathic

generalized epilepsy with typical absences and either the patient or a caregiver could keep a seizure diary. Patients with an implanted device, for example, a vagus nerve stimulator, were excluded from this study due to possible interference of magnets with the SD device. Written informed consent was obtained from every participant. The ethical committee of UZ/KU Leuven approved this study.

2.2 | Data collection

Patients underwent video-EEG monitoring (Schwarzer EEG amplifier, O.S.G.) using the standardized 25-electrode array of the International Federation of Clinical Neurophysiology.[20] Behind each ear, two additional Ag/AgCl cup electrodes (Ambu Neuroline cup, Ambu) were attached on the mastoid bone for concomitant recording with the SD. The closest corresponding electrodes on 25-channel EEG were T7 and T8 for the top electrode and P9 and P10 for the lower electrode. The SD, a small device of 24.5 × 33.5 × 7.73 mm and 6.3 g, was attached on the upper back using a patch (Figure 1), and two bipolar channels were created by connecting the ipsilateral top and lower electrode. Impedance was ≤5 kΩ at the beginning and checked throughout. The sampling rate of the SD and video-EEG was 250 Hz. Battery life and memory storage of the SD were 24 h and 2 Gb, respectively.

During their 24-h EMU stay, patients and caregivers (for pediatric patients) were also asked to report experienced absences in a seizure diary.

2.2.1 | *Clinical data analysis*

Comparison of SD to 25-channel EEG

BrainRT (O.S.G.) was used for the visualization of the EEG data. The 25-channel EEG was annotated for adults (W.V.P.) and children (K.J.). Five experienced epileptologists (A.V.D., C.D., E.V., L.Se., and W.V.P.) annotated the two-channel SD EEG blinded to clinical and 25-channel EEG data. In both EEG datasets, the onset and end of all 3-Hz generalized SWDs, lasting 3 s or more, were marked. We will refer to these annotations as "absences". Examples of absences on the SD are shown in Figure 2.

First, to match the SD annotations to the ground truth EEG annotations, alignment of the SD data with the 25-channel EEG was needed. In addition to the easily removable constant offset between the two devices, clock drifts or jitters may cause nonstable misalignment. Two different clocks on the devices cause clock drifts. Even when the initial offset is removed, as time passes, the difference between the two clocks will result in an increase in misalignment. In our case, the drift was random, meaning that it cannot be corrected for. We noted that the maximum drift is around 3 s/h. Furthermore, jitters are random variations in the timing offset from measurement to measurement. Instead of using time warping methods,[21] in view of their high complexity, we proposed and used an alternative method, based on the computation of the cross-correlation of the two signals in segments. After resampling the SD at the same frequency as the 25-channel EEG and removing the first 5 min (which are usually of lower quality), we performed the alignment in 1-h segments. First, we removed the initial onset. The cross-correlation of the first 3 h was computed, and the entire signal was moved to obtain maximal correlation for this segment. Then, we computed the cross-correlation of each 1-h segment with the respective segment in the 25-channel EEG, sequentially. Each segment was moved to obtain the maximum correlation; all the following segments were moved with the same number of samples. After applying this method, the mean absolute misalignment that may occur over the entire duration of the signal was 600 ms. If we segment the signal into smaller (<1 h) windows, the mean absolute misalignment can be further decreased at the expense of computation time.

Performance metrics: clinical validation

We compared the annotations of absences on the 25-channel EEG and SD. Annotation of an overlapping absence on both datasets was considered a true positive (TP). Annotation of an absence on 25-channel EEG, but not on SD was considered a false negative (FN). Annotation of an absence on SD, but not on 25-channel EEG was considered a false positive (FP). The primary outcomes were sensitivity, precision, and F1 score of the SD. Sensitivity of SD recordings evaluates how many seizures were successfully identified and was calculated as follows: TP / (TP + FN). Precision of seizure detection was computed using the following formula: TP / (TP + FP); this determines whether a seizure detected on SD is an actual seizure. Finally, the accuracy of the SD in comparison to the 25-channel EEG was measured using the F1 score: 2 × (precision × sensitivity) / (precision + sensitivity), giving a value between 0 (poor) and 1 (excellent). This analysis was performed for each epileptologist, and the median performance across epileptologists was calculated.

To evaluate interrater reliability, the intraclass correlation coefficient and 95% confidence intervals were measured, using SPSS version 27 (IBM). A mean rating ($k = 5$), absolute agreement, two-way random effects model was used.

Patient self-reporting of seizures in a seizure diary was analyzed in relation to seizure detection on 25-channel EEG. Sensitivity, precision, and F1 score of self-reporting were calculated. If the patient reported an event within 5 min after

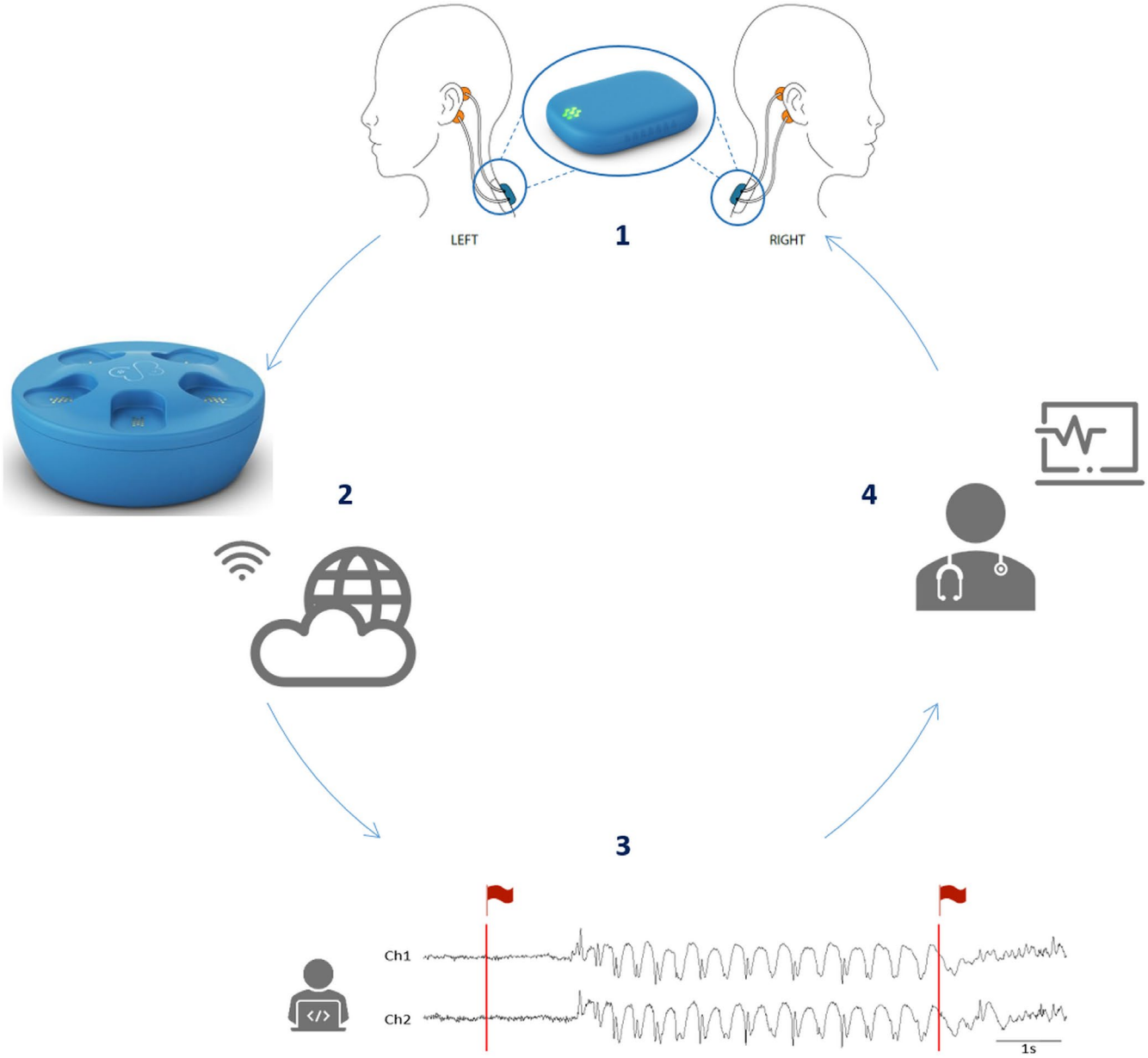

FIGURE 1 Concept of the Sensor Dot (SD) used as a wearable to detect absence seizures. (1) Four electrodes (in orange) are placed behind the ears of the patient and connected to the mobile electroencephalographic (EEG) device, the SD, which is attached to the upper back via an adhesive (in blue). An enlarged image of the SD is given in the circle. (2) After 24 h of recording, the SD is placed in the docking station, which allows recharging of the battery. In addition, when the SD is in the docking station, the SD EEG data are automatically uploaded to the cloud via a Wi-Fi connection. (3) Afterward, the absence detection algorithm analyzes the data and flags segments of interest (in red). (4) Finally, the flagged data are sent back to the treating neurologist, who can then review the flagged SD EEG data in a short time.

the actual seizure, this was defined a TP. A Mann–Whitney *U* test was performed for nonnormally distributed data.

2.2.2 | *Automatic analysis with machine learning algorithm*

We also propose a personalized semiautomatic seizure detection algorithm for detecting absences on SD EEG. The data with the algorithm-flagged regions were presented to the epileptologists, who only needed to decide whether the flagged segment was an actual seizure or an FP, leading to a reduction in review time (Figure 1). The machine learning (ML) algorithm was implemented in MATLAB 2017 and the built-in function, therein, for the training of support vector machines (SVMs).

Performance metrics: Validation of algorithm

The following metrics were applied to determine the performance of the seizure detection algorithm (following the definitions in Vandecasteele et al.[22]):

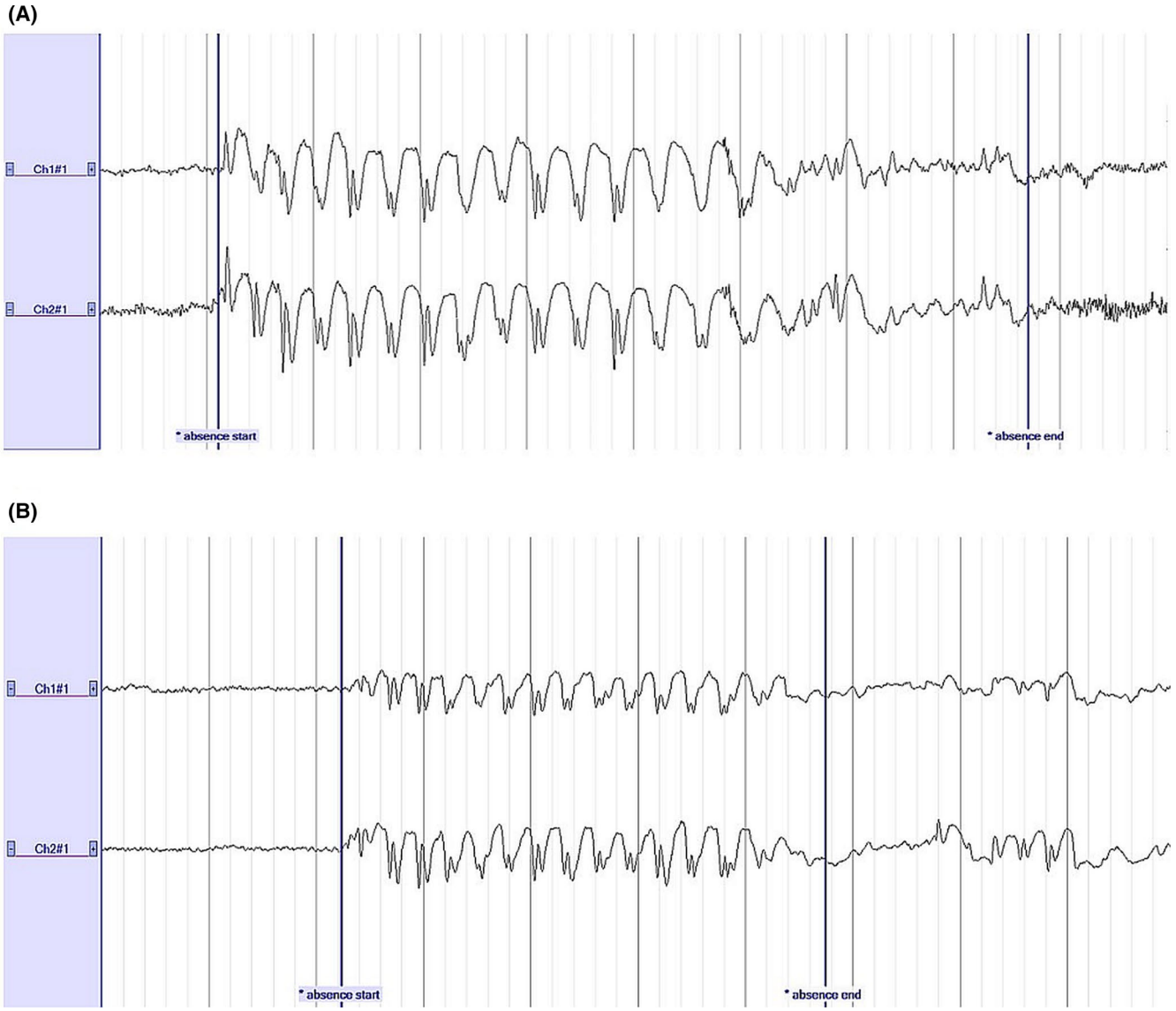

FIGURE 2 Examples of 3-Hz spike-and-wave discharges visible on the two-channel Sensor Dot during an absence seizure in (A) a pediatric patient and (B) an adult patient. A high-pass filter of .53 Hz, a low-pass filter of 35 Hz, and a notch filter were applied. Sensitivity: 100 μV/cm. Time base: 10 s. Absences lasting 8 s (A) and 5 s (B) were marked. Ch1#1, left; Ch2#1, right

1. Detection sensitivity: $TP/TP + FN$. A seizure was detected correctly (TP) if the detection occurred between the EEG onset and end of the seizure.
2. FP per hour. FPs within 10 s of each other were counted as one FP.

We will not report specificity measures, because for all cases the specificity was >99%, due to the highly imbalanced classes (the class of background EEG is dominant compared to the class of seizure segments).

Subsampling for balancing the classes

As a basis for designing our algorithm, the algorithm proposed by Kjaer et al.[23] was used, which is one of the very few algorithms designed for single channel absence seizure detection. We noticed that this algorithm suffered from stability issues, as the standard deviations of the sensitivity and the false alarm rate were high, mainly arising from the random selection of background samples for balancing the classes. We, therefore, exploited different undersampling approaches and opted for the use of an adapted version of the cluster-based undersampling approach proposed by Yen and Lee.[24] The number of background samples, N_k, selected from each cluster k was equal to $N_k = mS_s\frac{S_{b_k}}{S_b}$. We defined m as the ratio between the background and seizure samples we aimed to obtain in our training set, K as the number of clusters on which we clustered all the background samples, and S_s, S_b, S_{b_k} as the total number of seizure samples, the total number of background samples, and the number of

background samples in the k cluster, respectively. A detailed analysis on how the selection of the number of clusters, K, affected the performance of the subsampling can be found in Yen and Lee.[24] In this study, m was set equal to 25 and $K = S_s$.

Preprocessing and feature calculation

Each SD channel was filtered with a bandpass filter (1–25 Hz). Subsequently, the data were segmented in 2-s windows with 50% overlap and features were calculated for each.

We tried to improve the performance obtained from the features used in Kjaer et al.[23] by adding the features used in Vandecasteele et al.[22] (and the use of the aforementioned subsampling method). To select the subset of the features used in Vandecasteele et al.,[22] we performed a feature selection with random forests.[25] Features 1, 3, and 11 represent the extra features added to those of Kjaer et al.[23] The cross-correlation Features 2 and 10 were not normalized to lag 0 (contrary to those used in Kjaer et al.[23]), because we noticed that this normalization decreased their discriminative power. Our final feature set is given in Table 1.

The 13 different features were extracted from each window and each channel separately. Due to the subject-dependent differences in the amplitude of the EEG over time, normalization of the features was needed to achieve optimal detection of seizure events. We have used the median decaying memory as the optimal normalization method for line length features.[26]

Classification of seizure segments

A weighted SVM with a radial basis function kernel was used as classifier. Although a cluster-sized subsampling method was used for balancing the clusters, the ratio m was not set to 1 but equal to 25, which is why the weighted version of the classifier was used. The weights given to each nonseizure and seizure data point were $\frac{N+S_s}{2*N}$ and $\frac{N+S_s}{2*S_s}$, respectively, with N being the number of background samples selected during the subsampling and S_s the total number of seizure points. The number of seizures per patient (for the majority) was not enough to allow having both a training set, to employ cross-validation with k-folds, and a separate test set. When partitioning the available data into three sets (test, validation, and training), the number of seizures that could be used for learning the model would have been drastically reduced, and the results might be highly affected by the random choice of the pair of (train, validation) sets. Hence, we opted for nested k-fold cross-validation.[27,28] The cross-validation approach used was leave-one-seizure-out, if the subject had a maximum number of 10 seizures. For 10–19 seizures, we created folds with two seizures each; for 20–29 seizures, we created folds with three seizures each, et cetera. The fold splits were set exactly in the middle of the nonseizure data between two seizures.

TABLE 1 Feature set of the machine learning algorithm

Time domain	(1) Zero crossings
	(2) Cross-correlation between two consecutive windows
	(3) Root mean square error amplitude
Frequency domain	(4) Power of the signal in frequency band 1–30 Hz
	(5) Relative power of the signal between bands 3–12 Hz and 1–30 Hz
	Log-sum of wavelet transform after resampling at 128 Hz: (6) 32–64 Hz, (7) 16–32 Hz, (8) 8–16 Hz, (9) 2–4 Hz
	(10) Cross-correlation of same window in two different bands, 3–12 Hz and 1–30 Hz
	(11) Dominant phase
	(12) Mean phase variance
	(13) Mahalanobis variance between each point of the 3–12-Hz band and 1–30 Hz

The hyperparameters were optimized per fold. The values of the hyperparameters of the SVM model (C and gamma) were selected using a fivefold cross-validation of the "fold-training set" (in a nested-cross validation scheme). The values that resulted in the maximum sensitivity were selected (in our use-case, we were looking for maximum sensitivity to mark all possible events, after which they were reviewed by an epileptologist). Hence, the hyperparameter search is not likely to overfit the dataset, as it is only exposed to a subset of the dataset provided by the outer cross-validation procedure. In the "inner k-fold split" we optimized the hyperparameters, and in the "outer k-fold split" we estimated the generalization error.

Postprocessing

We tested two versions of the algorithm. In the first version, an alarm for seizure detection was given when two consecutive windows were noted as seizures. In the second version, an alarm for seizure detection was given when three consecutive windows were noted as seizures. Furthermore, in the second version (hereinafter called "postprocessed version"), whenever two seizures (of three windows each) were separated only by one nonseizure window, they were merged.

Clinical validation

Six epileptologists (A.V.D., C.D., J.M., L.Se., E.V., and W.V.P.) reviewed the files containing the labels made by the postprocessed version of the algorithm, and performance was again calculated.

3 | RESULTS

3.1 | *Study characteristics*

We included 12 patients with typical absence seizures, of whom eight were adult and four were pediatric patients (median age = 21 years, range = 8–50 years, seven female). Further patient details are given in Table 2. Total recording time was 237 h, 11 min, and 21 s. The median recording time for a patient was 20 h, 28 min, and 22 s (range = 13:36:05–21:38:47). In these 12 patients, we recorded 284 absences on 25-channel EEG (Table S1). We obtained a median of 13 absences (range = 2–81), and a median seizure duration of 5 s (range = 3–22 s).

3.2 | *Review of full SD EEG recording*

We report median performance across five epileptologists presented in an ascending order based on their score. A median sensitivity of .81 (range = .52–.84) and median precision of .89 (range = .53–.97) was obtained. Ultimately, a median F1 score of .73 (range = .63–.90) was obtained. Sixteen occurrences of correctly annotated absences on SD were present on 25-channel EEG but not annotated. After revision by an epileptologist (W.V.P.), we corrected the 25-channel EEG annotation and rated the SD annotation as TP. The majority of FPs on SD were due to chewing artifacts (in 72% of all cases; Figure 3A). Alternatively, seizures were usually missed because of signal distortion due to muscle artifacts and poor EEG quality (Figure 3B,C).

3.2.1 | Interrater reliability

An intraclass correlation coefficient of .642 with a 95% confidence interval of .564–.709 was obtained, which corresponds to moderate interrater reliability.

3.2.2 | SD performance metrics of seizures with a duration of ≥4 s

We observed that a large number of seizures lasting 3 s on the 25-channel EEG had a shorter duration on the SD and hence were missed (Figure S1). We removed all seizures of 3 s and recalculated the performance metrics to observe potential influence. A median sensitivity of .86 (range = .56–.88), precision of .88 (range = .51–.97), and F1 score of .76 (range = .64–.92) was obtained.

3.3 | *Results and review of algorithm-labeled files*

The three automated absence detection algorithms (Kjaer et al., our initial, and our postprocessed version of the algorithm) were tested on the data of the 12 subjects. Results of these algorithms for each subject are presented in Table S2. Every algorithm ran 30 times. Kjaer's algorithm had a sensitivity of .9503 and FPs/h of 3.1281. The initial version of the algorithm outperformed it both in sensitivity and in FPs/h rate, with .9967 and 2.3929, respectively. The postprocessed version significantly decreased the FPs/h rate to .9138 with a concomitant small drop in sensitivity to .983.

Because the postprocessed version detected >98% of absences on the SD EEGs, with approximately 62% fewer FP detections in comparison with the first version, we selected this algorithm for further study. We presented the algorithm-labeled SD EEG files to the epileptologists for visual review of seizures. A median sensitivity of .83 (range = .77–.88), precision of .89 (range = .70–.99), and F1 score of .87 (range = .73–.89) was obtained. Although the medians of sensitivity and precision did not change considerably, the ranges were narrower due to fewer lower scores. The average time to review a 24-h, algorithm-labeled SD EEG file was 5–10 min, in comparison to 1–2 h for full EEG review without automated annotations.

3.4 | *Performance of patient self-reporting*

Self-reporting by patients or caregivers in seizure diaries was compared to the seizures detected on 25-channel EEG. Seizure diary data were missing for one patient. Seven of 11 patients reported zero absence seizures during the 24-h recording, although they had on average 19 absences. Only three of 11 reported absences, of whom two were pediatric patients and seizure reporting was done by a caregiver. Patients or caregivers reported 6% of the 3-Hz SWDs lasting between 3 and 6 s and 14% of the 3-Hz SWDs lasting longer than 6 s (Figure 4). Seizures that were reported had a significantly longer duration (7 s, range = 3–15 s) than unreported seizures (5 s, range = 3–22 s; $p = .001$). Over 11 patients, a sensitivity of .08, precision of 1.00, and F1 score of .15 were obtained.

4 | DISCUSSION

We showed that typical absence seizures can be accurately detected (F1 score = .73) using an unobtrusive EEG-based wearable with only two behind-the-ear channels. Visual

TABLE 2 Patient characteristics

Subjects	Sex	Age, years	Age at onset, years	Familial history	Epilepsy syndrome	EEG pattern	Current AEDs	Past AEDs
SUBJ-1	F	50	22	No	JAE (A, GTCS)	3 Hz GSW, GPSW	VPA 2 × 500 mg, TPM 2 × 50 mg	CBZ, LTG, ESM, LCM, CLB, VGB, CZP
SUBJ-2	M	9	8	Yes	CAE (MS, A)	3 Hz GSW	TPM 2 × 200 mg, VPA 2 × 300 mg, CZP 3 × 2.5 mg/ml	ESM
SUBJ-3	M	19	6	No	JAE (A, GTCS)	3–4 Hz GPSW	LCM 200 mg, VPA 1 g	CBZ, ESM, LTG
SUBJ-4	F	9	8	No	CAE (A)	3 Hz GSW	VPA 2 × 300 mg	ESM, LTG
SUBJ-5	F	25	6	Yes	JAE (A, GTCS, MS)	3 Hz GSW	BRV 2 × 50 mg, CZP 3 × .5 mg, LTG 200–300 mg	ESM, LEV, VPA
SUBJ-6	F	44	12	No	JAE (A, GTCS)	3 Hz GSW, GPSW	CZP .5 mg, LCM 300 mg, VPA 1500 mg	ESM, LEV, LTG, TPM
SUBJ-7	F	21	13	Yes	JAE (A, GTCS)	3 Hz GSW, GPSW	CLB 3 × 10 mg, LCM 2 × 200 mg	CZP, ESM, LEV, LTG, VPA
SUBJ-8	F	20	12	No	JAE (A, GTCS)	3-4 Hz GSW, GPSW	LTG 2 × 300 mg, ESM 250 mg	LEV
SUBJ-9	M	22	15	Yes	JAE (A, GTCS)	3-4 Hz GSW, GPSW	VPA 300 mg, LTG 2 × 200 mg, ESM 2 × 10 ml/d, LCM 2 × 100 mg	LEV
SUBJ-10	M	24	10	No	JAE (A, GTCS)	3 Hz GSW, GPSW	LTG 2 × 200 mg, VPA 1 g	CZP, ESM, LEV, OXC, TPM, PER, LCM, BRV
SUBJ-11	M	12	8	No	JME (A, GTCS)	3 Hz GSW	VPA 2 × 300 mg	–
SUBJ-12	F	8	7	No	JAE	3 Hz GSW	VPA 2 × 5 ml, LEV 2 × 3.5 ml	–

Abbreviations: A, absence; AED, antiepileptic drug; BRV, brivaracetam; CAE, childhood absence epilepsy; CBZ, carbamazepine; CLB, clobazam; CZP, clonazepam; EEG, electroencephalographic; ESM, ethosuximide; F, female; GPSW, generalized polyspike waves; GSW, generalized spike waves; GTCS, generalized tonic–clonic seizures; JAE, juvenile absence epilepsy; JME, juvenile myoclonic epilepsy; LCM, lacosamide; LEV, levetiracetam; LTG, lamotrigine; M, male; MS, myoclonic seizures; OXC, oxcarbazepine; PER, perampanel; TPM, topiramate; VGB, vigabatrin; VPA, valproate.

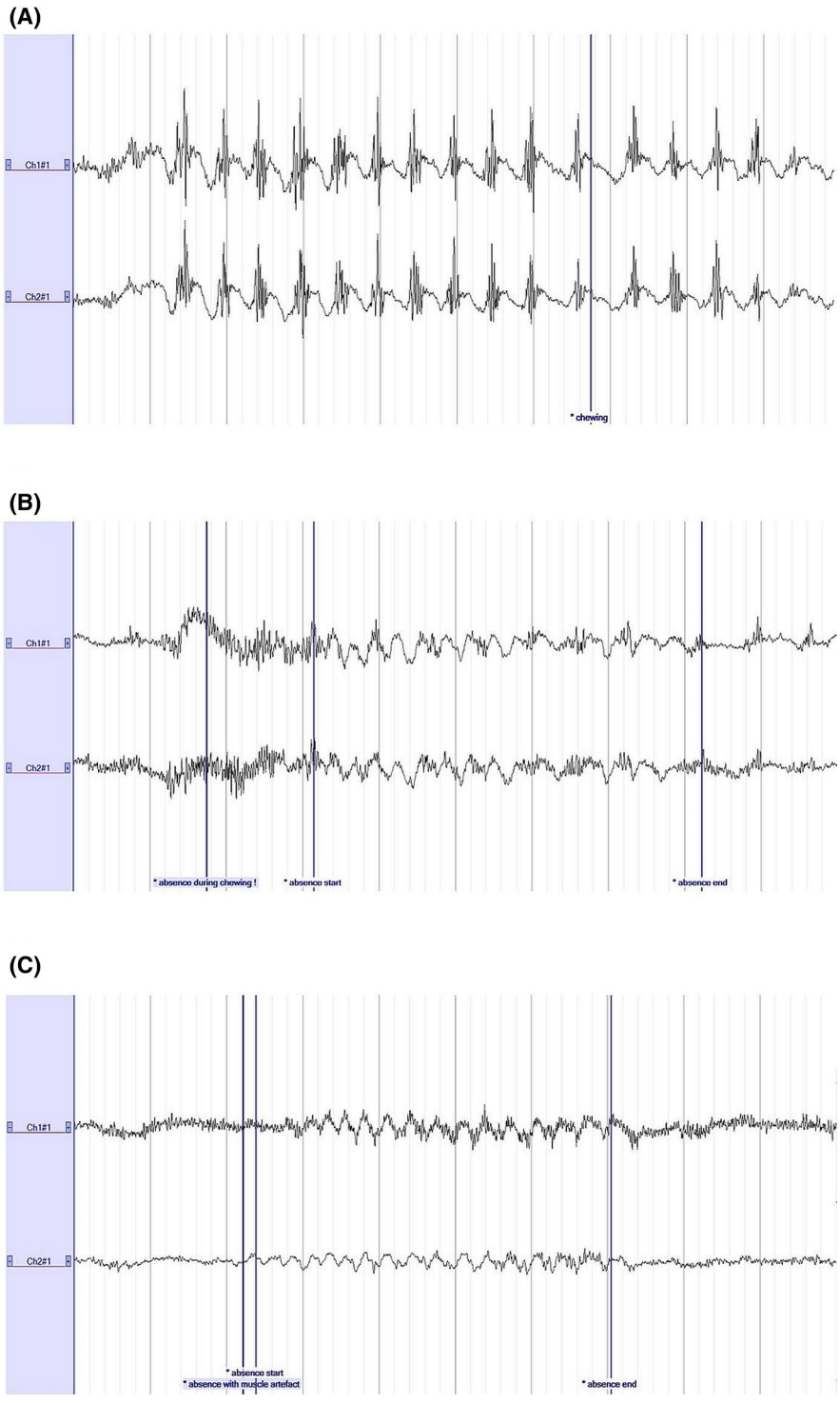

FIGURE 3 Common reasons for a false positive (FP) or false negative (FN) annotation on Sensor Dot. (A) Chewing artifact, characterized by 2-Hz slow waves with superimposed muscle artifacts, which were often mistaken for seizures (FPs). (B, C) Commonly missed absences due to the presence of chewing artifacts (B) and muscle artifacts (C). A high-pass filter of .53 Hz, a low-pass filter of 35 Hz, and a notch filter were applied. Sensitivity: 100 μV/cm. Time base: 10 s. Ch1#1, left; Ch2#1, right

review of the SD EEG files, annotated with our automated absence detection ML algorithm, suggested an even better result (F1 score = .87) with a review time of only 5–10 min.

The situation of patients with refractory absence epilepsy may be improved by optimizing antiepileptic drugs. However, the current basis for therapeutic decision-making, namely the seizure diary, lacks objectivity. Because of the ability to accurately quantify 3-Hz SWDs, the benefits of long-term EEG monitoring to document the response to absence treatment had already been reported more than 25 years ago.[29,30] Long-term EEG monitoring using current equipment is obtrusive, usually limited to 24 h, and often performed in the hospital. Currently, the SD may allow for long-term unobtrusive, user-friendly monitoring at home and offers a new and complete framework to ensure clinical adoption, as is shown in Figure 1. Although the accuracy is not perfect, absences usually occur very frequently, and therefore it seems that this will

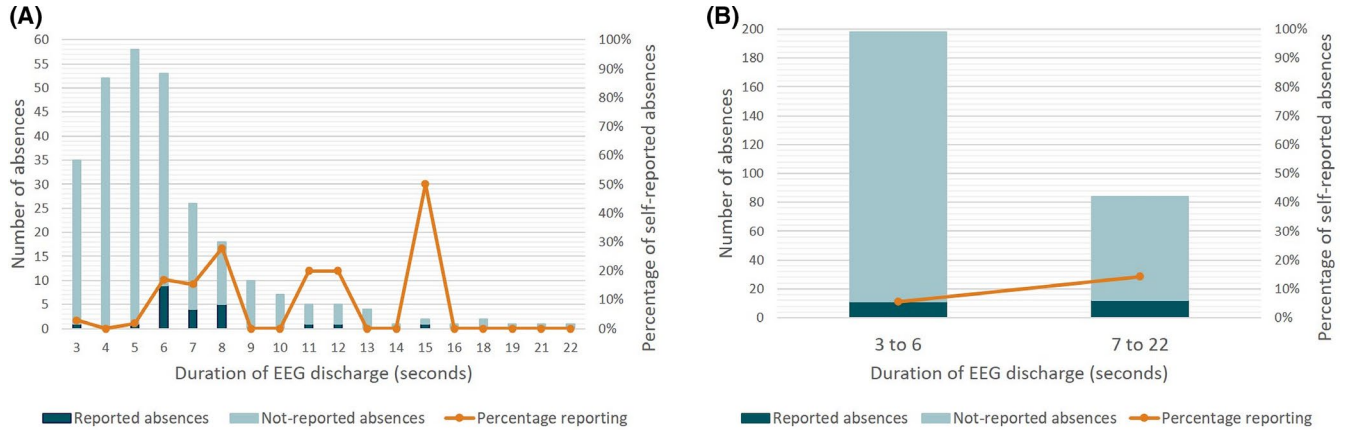

FIGURE 4 Percentage of seizures (defined in this study as a discharge lasting 3 s or longer) of different duration reported by the patients themselves or by caregivers for children. (A) Each duration separately. (B) Grouped into shorter and longer duration in relation to the findings by Guo et al.[31] EEG, electroencephalographic

not significantly influence the outcome. Furthermore, our algorithm requires confirmation by a physician. Although some neurologists might not prefer this approach, others like to visually interpret the EEG and propose a therapy based on seizure frequency as well as waveform. By contrast, implementing a fully automated seizure detection would require an algorithm with a low computational power that can run locally on the SD, which is not yet feasible.

Typical absence seizures are characterized by abrupt impaired awareness and brief interruption of activities, with generalized 3-Hz SWDs on EEG. In our study, we defined an absence as having the latter characteristics on EEG for at least 3 s. This was done for research purposes only, considering that we aimed to study whether these typical EEG patterns would be equally recognizable using only two channels. A 3-s 3-Hz SWD might not always have a clinical correlate. Guo et al.[31] found that 3-Hz SWDs with impaired behavior had on average a longer duration than 3-Hz SWDs without impaired behavior (7.9 $\pm$ 6.6 s vs. 3.8 $\pm$ 3.0 s). It was actually the power on EEG and functional magnetic resonance imaging, and thus the intensity of physiological changes, at seizure onset that was associated with impaired behavior. This means that shorter 3-Hz SWDs may also have a clinical correlate, and that it is not possible to determine whether an absence was present merely based on 3-Hz SWD duration.

In this study, we confirmed the well-known issue of absence seizure underreporting. Even patients with 3-Hz SWDs lasting 7 s or longer underreported their absences in 86% of all cases. Unreported seizures typically had a shorter duration (5 s) than seizures that were picked up by patients or caregivers (7 s), which is in line with the observation by Guo et al.[31] that seizures with impaired behavior usually have a longer duration. Interestingly, the precision of reported absences was 100%; that is, none of the patients reported an absence without concomitant 3-Hz SWD on EEG. From our data, the reason for this underreporting is unclear and warrants further study. In contrast to the seizure diary, the SD clearly reflected more accurately the actual seizure occurrence. As shorter absences arguably do not have a clinical correlate, patient underreporting remains a major issue even when absences lasted long enough to probably change behavior and consequently be picked up by someone. Because the SD EEG is an objective measure of 3-Hz SWD frequency and duration, it will bypass several of the problems with seizure diaries, such as unawareness of seizures, noncompliance, and inaccurate sensitivity.

We showed that typical absence seizures can be detected using the SD, with a sensitivity of .83; that is, 17% of 3-Hz SWD lasting 3 s or longer on the 25-channel EEG were missed on SD EEG and represented FNs. Common reasons for FNs were artifacts. When using only two EEG channels, the presence of artifacts might distort the entire signal, whereas on 25-channel EEG patterns might still be visible on the remaining leads. Another reason for not annotating absences on SD EEG was the location of the electrodes behind the ear. We choose this location to make the device as unobtrusive as possible. However, the best location to record 3-Hz SWDs is in the frontal regions.[32,33] The duration of 3-Hz SWDs on SD EEG was frequently somewhat shorter compared to the 25-channel EEG, which also covered the frontal regions (Figure S1).

Furthermore, typical absences were detected with a precision of .89; that is, only 11% of 3-Hz SWDs lasting 3 s or longer annotated on SD were not present on the 25-channel EEG and represented FPs. The majority of FPs were due to chewing artifacts, which resemble the SWD pattern. However, this chewing artifact is distinguishable

from 3-Hz SWD by its frequency (around 2 Hz), with superimposed muscle artifacts.

The SD data were read blindly twice by several neurologists, first the full SD EEG file and second the algorithm-labeled SD EEG file. We noticed that both sensitivity and precision increased when the data were reviewed a second time, which in our view reflects a learning curve in reading behind-the-ear SD EEG. We speculate that it is a matter of familiarization with the signals and that overall performance will increase as readers gain more experience in reviewing SD data. It is also possible that the data reduction implemented by the automated algorithm allowed a shorter and more focused review, leaving less room for human error.

The proposed algorithm exhibited a significant difference in sensitivity to Kjaer's algorithm,[23] which was mainly due to the cluster-size subsampling method used for the balancing of the classes. We have shown that the use of a seizure detection algorithm is timesaving in reviewing 24-h SD EEG files of patients with typical absences. Our algorithm is patient-specific, and hence data from each new patient are needed to retrain the algorithm. Practically, the first phase will consist of routine monitoring in the EMU, after which these data can be used to train the algorithm. The patient can then wear the SD at home. We argue that the time needed for annotating the hospital data is limited compared to the time needed for annotating extensive recordings in the home environment. Furthermore, we believe that the increased performance of a patient-specific approach justifies the time needed to annotate a small portion of the hospital data of each patient.

According to the standards for testing and clinical validation of seizure detection devices,[34] our study is classified as a Phase 2 study,[34] because the SD was validated in 12 in-hospital patients (although we recorded 284 seizures) at only one center with subsequent offline analysis. We plan a Phase 4 study, in which the accuracy and usability of the SD in a home environment will be investigated in a multicenter trial (EIT Health: SeizeIT2; clinicaltrials.gov: NCT04284072).[19]

The wearable, unobtrusive SD has the potential to become a game-changing medical device in the management and research of patients with typical absences.

ACKNOWLEDGMENTS

This study was supported by EIT Health Grant 21263–SeizeIT2: Discreet Personalized Epileptic Seizure Detection Device. SeizeIT started out as an imec.icon research project (2016–2019), and currently continues as an EIT Health-funded initiative (2020–2021). Project partners are KU Leuven, UCB Pharma, Byteflies, PiliPili, Neuroventis, Karolinska Institute, Aachen UMC, UH Freiburg, Oxford University Hospitals NHS, King's College London, and CHUC Coimbra. This research received funding from the Flemish Government under the "Onderzoeksprogramma Artificiële Intelligentie (AI) Vlaanderen" program.

CONFLICT OF INTEREST

L.L. has received speaker honoraria from and is participating on advisory boards for Zogenix, Livanova, UCB, Eisai, Novartis, NEL, and Epihunter. None of the other authors has any conflict of interest to disclose. We confirm that we have read the Journal's position on issues involved in ethical publication and affirm that this report is consistent with those guidelines.

ORCID

Lauren Swinnen https://orcid.org/0000-0003-0531-9101
Lieven Lagae https://orcid.org/0000-0002-7118-0139
Chantal Depondt https://orcid.org/0000-0002-8452-5319
Jaiver Macea https://orcid.org/0000-0002-7645-897X
Kaat Vandecasteele https://orcid.org/0000-0002-9888-577X
Wim Van Paesschen https://orcid.org/0000-0002-8535-1699

REFERENCES

1. Commission on Classification and Terminology of the International League Against Epilepsy. Proposal for revised clinical and electroencephalographic classification of epileptic seizures. Epilepsia. 1981;22(4):489–501.
2. Guilhoto LM. Absence epilepsy: continuum of clinical presentation and epigenetics? Seizure. 2017;44:53–7.
3. Scheffer IE, Berkovic S, Capovilla G, Connolly MB, French J, Guilhoto L, et al. ILAE classification of the epilepsies: position paper of the ILAE Commission for Classification and Terminology. Epilepsia. 2017;58(4):512–21.
4. Antwi P, Atac E, Ryu JH, Arencibia CA, Tomatsu S, Saleem N, et al. Driving status of patients with generalized spike–wave on EEG but no clinical seizures. Epilepsy Behav. 2019;92:5–13.
5. Kessler SK, McGinnis E. A practical guide to treatment of childhood absence epilepsy. Pediatr Drugs. 2019;21(1):15–24.
6. Grosso S, Galimberti D, Vezzosi P, Farnetani M, Di Bartolo RM, Bazzotti S, et al. Childhood absence epilepsy: evolution and prognostic factors. Epilepsia. 2005;46(11):1796–801.
7. Callenbach PMC, Bouma PAD, Geerts AT, Arts WFM, Stroink H, Peeters EAJ, et al. Long-term outcome of childhood absence epilepsy: Dutch Study of Epilepsy in Childhood. Epilepsy Res. 2009;83(2–3):249–56.
8. Holtkamp M, Janz D, Kirschbaum A, Kowski AB, Vorderwülbecke BJ. Absence epilepsy beyond adolescence: an outcome analysis after 45 years of follow-up. J Neurol Neurosurg Psychiatry. 2018;89(6):603–10.
9. Elger CE, Hoppe C. Diagnostic challenges in epilepsy: seizure under-reporting and seizure detection. Lancet Neurol. 2018;17(3):279–88.
10. Akman CI, Montenegro MA, Jacob S, Eck K, Chiriboga C, Gilliam F. Seizure frequency in children with epilepsy: factors influencing accuracy and parental awareness. Seizure. 2009;18(7):524–9.
11. Keilson MJ, Hauser A, Magrill JP, Tepperberg J. Ambulatory cassette EEG in absence epilepsy. Pediatr Neurol. 1987;3:273–6.

12. Fiest KM, Birbeck GL, Jacoby A, Jette N. Stigma in epilepsy. Curr Neurol Neurosci Rep. 2014;14(5):444.
13. Ryvlin P, Beniczky S. Seizure detection and mobile health devices in epilepsy: recent developments and future perspectives. Epilepsia. 2020;61:1–2.
14. Zibrandtsen IC, Kidmose P, Christensen CB, Kjaer TW. Ear-EEG detects ictal and interictal abnormalities in focal and generalized epilepsy—a comparison with scalp EEG monitoring. Clin Neurophysiol. 2017;128(12):2454–61.
15. Zibrandtsen IC, Kidmose P, Kjaer TW. Detection of generalized tonic-clonic seizures from ear-EEG based on EMG analysis. Seizure. 2018;59:54–9.
16. Frankel MA, Lehmkuhle MJ, Watson M, Fetrow K, Frey L, Drees C, et al. Electrographic seizure monitoring with a novel, wireless, single-channel EEG sensor. Clin Neurophysiol Pract. 2021;6:172–8.
17. Bruno E, Simblett S, Lang A, Biondi A, Odoi C, Schulze-Bonhage A, et al. Wearable technology in epilepsy: the views of patients, caregivers, and healthcare professionals. Epilepsy Behav. 2018;85:141–9.
18. Simblett SK, Biondi A, Bruno E, Ballard D, Stoneman A, Lees S, et al. Patients' experience of wearing multimodal sensor devices intended to detect epileptic seizures: a qualitative analysis. Epilepsy Behav. 2020;102:106717.
19. EIT Health. SeizeIT2: Discreet, personalised epileptic seizure detection device. 2020. https://eithealth.eu/project/seizeit2/. Accessed 8 April 2021.
20. Seeck M, Koessler L, Bast T, Leijten F, Michel C, Baumgartner C, et al. The standardized EEG electrode array of the IFCN. Clin Neurophysiol. 2017;128(10):2070–7.
21. Keogh EJ, Pazzani MJ, editors. Derivative dynamic time warping. International Conference on Data Mining. Chicago, IL: SIAM; 2001. p. 1–11.
22. Vandecasteele K, De Cooman T, Dan J, Cleeren E, Van Huffel S, Hunyadi B, et al. Visual seizure annotation and automated seizure detection using behind-the-ear electroencephalographic channels. Epilepsia. 2020;61(4):766–75.
23. Kjaer TW, Sorensen HBD, Groenborg S, Pedersen CR, Duun-Henriksen J. Detection of paroxysms in long-term, single-channel EEG-monitoring of patients with typical absence seizures. IEEE J Transl Eng Heal Med. 2017;5(2000):1–8.
24. Yen S-J, Lee Y-S. Cluster-based under-sampling approaches for imbalanced data distributions. Expert Syst Appl. 2009;36(3):5718–27.
25. Deviaene M, Testelmans D, Borzée P, Buyse B, Van Huffel S, Varon C, editors. Feature selection algorithm based on random forest applied to sleep apnea detection. In: Proceedings of the 41th Annual International Conference of the Engineering in Medicine and Biology Society (EMBC). Berlin, Germany; 2019. p. 1–4.
26. Logesparan L, Rodriguez-Villegas E, Casson AJ. The impact of signal normalization on seizure detection using line length features. Med Biol Eng Comput. 2015;53:929–42.
27. Filzmoser P, Liebmann B, Varmuza K. Repeated double cross validation. J Chemom. 2009;23(4):160–71.
28. Parvandeh S, Yeh HW, Paulus MP, McKinney BA. Consensus features nested cross-validation. Bioinformatics. 2020;36(10):3093–8.
29. Blomquist HK, Zetterlund B. Evaluation of treatment in typical absence seizures: the roles of long-term EEG monitoring and ethosuximide. Acta Paediatr Scand. 1985;74(3):409–15.
30. Appleton RE, Beirne M. Absence epilepsy in children: the role of EEG in monitoring response to treatment. Seizure. 1996;5:147–8.
31. Guo JN, Kim R, Chen YU, Negishi M, Jhun S, Weiss S, et al. Impaired consciousness in patients with absence seizures investigated by functional MRI, EEG, and behavioural measures: a cross-sectional study. Lancet Neurol. 2016;15:1336–45.
32. Crunelli V, Lőrincz ML, McCafferty C, Lambert RC, Leresche N, Di Giovanni G, et al. Clinical and experimental insight into pathophysiology, comorbidity and therapy of absence seizures. Brain. 2020;143(8):2341–68.
33. Duun-Henriksen J, Madsen RE, Remvig LS, Thomsen CE, Sorensen HBD, Kjaer TW. Automatic detection of childhood absence epilepsy seizures: toward a monitoring device. Pediatr Neurol. 2012;46(5):287–92.
34. Beniczky S, Ryvlin P. Standards for testing and clinical validation of seizure detection devices. Epilepsia. 2018;59:9–13.

SUPPORTING INFORMATION

Additional supporting information may be found online in the Supporting Information section.

How to cite this article: Swinnen L, Chatzichristos C, Jansen K, Lagae L, Depondt C, Seynaeve L, et al. Accurate detection of typical absence seizures in adults and children using a two-channel electroencephalographic wearable behind the ears. Epilepsia. 2021;62:2741–2752. https://doi.org/10.1111/epi.17061